Measurement of Velocity and Density Fields in a Supersonic Jet

Mehmet B. Alkislar, Luiz M. Lourenco and Anjaneyulu Krothapalli
Fluid Mechanics Research Laboratory
Department of Mechanical Engineering
Florida State University
2525 Pottsdamer Street
Tallahassee, Florida 32310

Introduction

In this study, the PIV technique is used to obtain accurate measurements of synoptic 2-D velocity and vorticity fields in the minor and major planes of a screeching jet, issuing from a rectangular nozzle. The detailed analysis of a stereoscopic PIV data set (Alkislar 2001) with conventional triple decomposition revealed dynamics of the coherent eddies which was previously discussed by Krothapalli *et. al* (2001). Strong coherent vortical structures were found to dominate the shear layer in the region of the screech sound generation. Since these vortical structures are the energy source of the screech feedback mechanism, it is important to assess the growth of instabilities in the initial region of the jet. The shear layer growth and turbulence characteristics of the flow field are the main indicators for the amplitudes of the instabilities in the flow field. Such an investigation was done for the mixing region of the jet by Krothapalli *et. al* (1986) by means of hotwire. However, the initial region and the effect of curvature in the shear layer imposed by the shock cell structure were not investigated previously, which is the focus of this study.

To complement the velocity field measurements the density field measurements were also obtained using an optical technique referred to as Laser Speckle Density (LSD).

Experimental setup

Experiments were conducted in the blow-down jet facility of the Fluid Mechanics Research Laboratory. This facility is capable of generating jets with Reynolds numbers

in excess of 3×10^6 with exit Mach numbers up to 2.15 and total temperatures up to 810 K. The M_d=1.44, convergent-divergent nozzle used in this study has a rectangular exit with 4:1 aspect ratio and 10 mm in short dimension.

Velocity Field Measurements

Velocity field data were obtained by means of PIV measurements. For this purpose Kodak ES1.0 CCD camera was used to take synoptic images of the flow field. The flow is seeded internally and externally with fine droplets of Rosco fog fluid. The internal seeding droplets are generated by a modified Wright nabulizer that produces particles with diameter of 0.1-1 μm, whereas the external seeding droplets, ranging 1-10 μm in diameter, are produced by Rosco 1600 Fog Generator.

The seeding particles in the flow are illuminated by a dual cavity, frequency doubled Nd-Yag laser (Spectra-Physics PIV-400) that is synchronized with the camera. To obtain optimum displacement between the particle images, the time, *Dt*, between the two laser pulses is kept in 0.8-2 μsec range. The acquisition of flow images is triggered by a signal generated by a frequency tracker, which locks on the fundamental screech frequency obtained from a near field microphone.

The velocity is computed using a novel mesh-free, second order accurate, processing algorithm suggested by Lourenco and Krothapalli (1998). This algorithm designed to improve the accuracy and spatial resolution of conventional cross-correlation schemes. The interrogation regions consist of particle images that have sizes ranging from 3 to 4 pixel squares. The high resolution and accuracy provide also higher order approximation to the derivatives of the velocity field and specifically the vorticity field.

Density Field Measurements

In order to complement the velocity, density field measurements were carried out using Laser Speckle Displacement method. The method is similar to the one suggested by Köpf (1972). As shown in **Figure 1** the laser source is expanded to illuminate the ground glass, which extends over the flow area of interest. The interference from the light scattered by the fine grain ground glass produces random speckle pattern. The size of the speckles depends on the aperture setting of the lens of the recording camera and the

wavelength of the laser light, and is of the order of 20-30 μm. When a flow field with a variable density, and thus variable index of refraction, $n(x,y,z)$, is inserted between the ground glass and the camera, the speckle pattern is displaced in the image plane at an amount of (Dx, Dy). This deflection of light by the presence of the medium is proportional to the gradient of refractive index. In the presence of jet flow, the refraction index is related to the gas density by the Gladstone-Dale constant, which dependents on the nature of the gas and the wavelength of the light propagating in the medium.

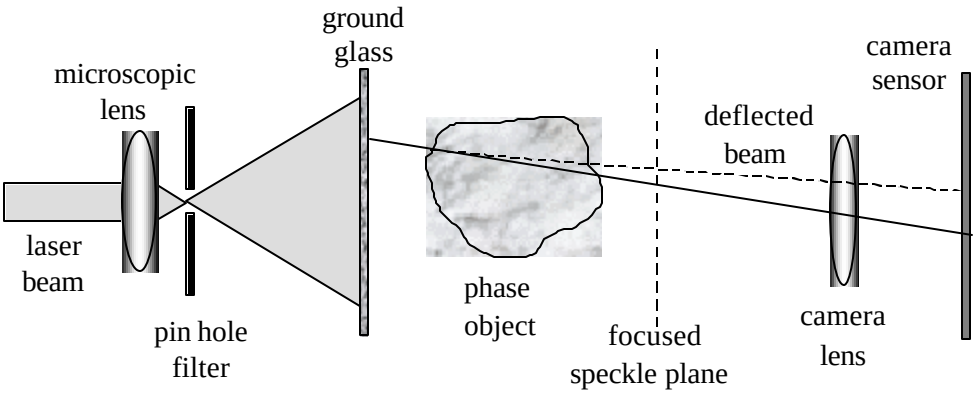

Figure 1. Illustration of Laser Speckle Method

Considering that the grains of the speckle pattern are like particles in a PIV image, it is possible to measure the speckle pattern displacement utilizing the same algorithms used in the processing of PIV pictures. The accuracy in the calculation of derivatives of displacements is also very important after the determination of displacement field, since this information is integrated to yield the density field of the flow.

A typical displacement field is given in **Figure 2**, which is processed by PIV cross correlation techniques, from the instantaneous speckle patterns. The figure shows the shock cell structure at the jet exit. The vectors in the figure shows how much and in what direction the density changes at the processed points.

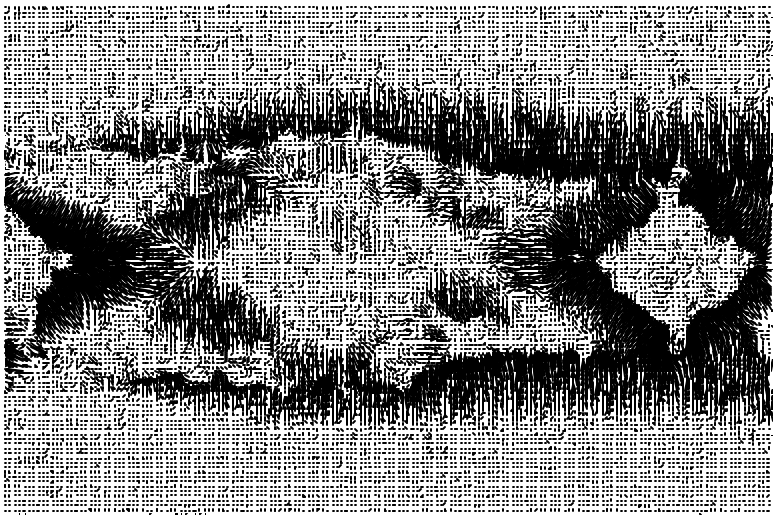

Figure 2. Displacement field of an instantaneous speckle pattern during the operation of the jet.

Evaluation of the density in the flow field

An integration method is proposed to have a solution where all points in the flow field are solved implicitly for the density. For this purpose, a Poisson equation is formed and solved for the density, where the measured quantities enter the equation as the source terms as given in Equation 1. The elliptic character of the equation ensure the contribution of every point to the solution, the smoothness of the solution and complete match of the boundary conditions of the density field.

$$\nabla^2 r = \frac{\partial^2 r}{\partial y^2} + \frac{\partial^2 r}{\partial y^2} = r_{xx} + r_{yy} = F(x, y) \tag{1}$$

The right hand side of the equation is the source function, *F(x,y)*, which consists of the measured quantities, r_{xx} and r_{yy}.

In order to get a unique solution the proper boundary conditions have to be applied. At the freestream boundaries of the domain, it is appropriate to use constant ambient density, $r = r_a$, and measured density gradient in the *x*-direction at the upstream and downstream boundaries, $\left.\frac{\partial r}{\partial x}\right| = r_x|_{measured}$.

In **Figure 3** the density field determined by the application of the Poisson equation to the displacement field of **Figure 2** is shown. The expansion and compression regions in the flow field can easily be identified with light and dark regions.

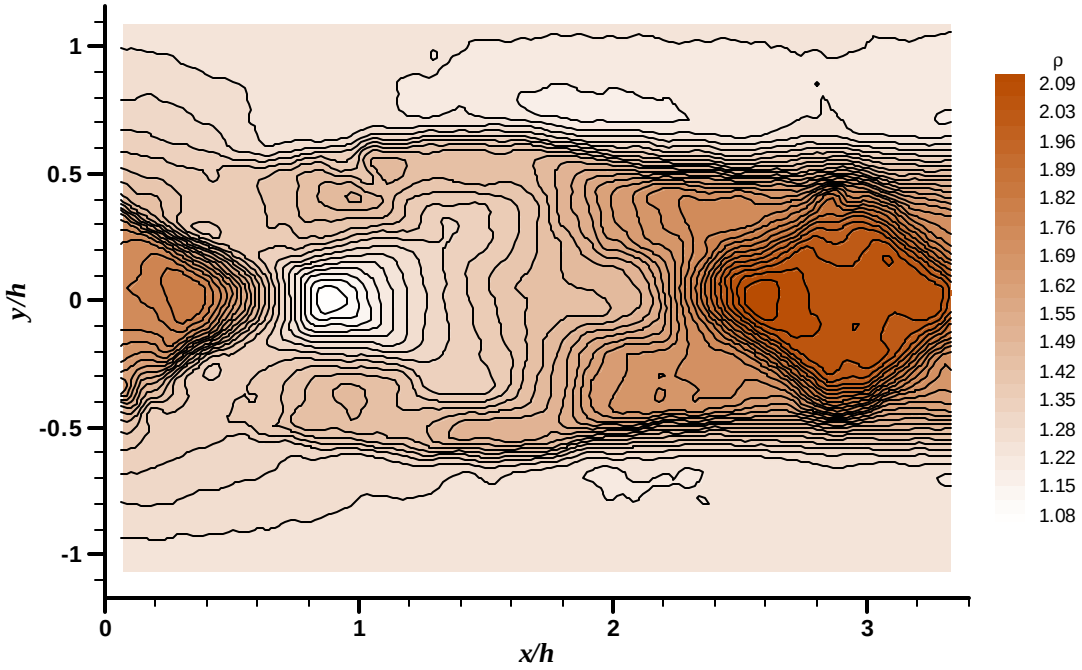

Figure 3. Density field of the instantaneous images shown in previous section after the application of Poisson equation.

Results and Discussion

The mean velocity field in the minor axis plane of jet with M_j=1.69 is presented in **Figure 4**. The region covered by the measurements extends from 0.1 h to 4.5 h in x direction, which encloses the first shock cell and one third of second shock cell. An ensemble of more than 600 realizations was used to obtain the results.

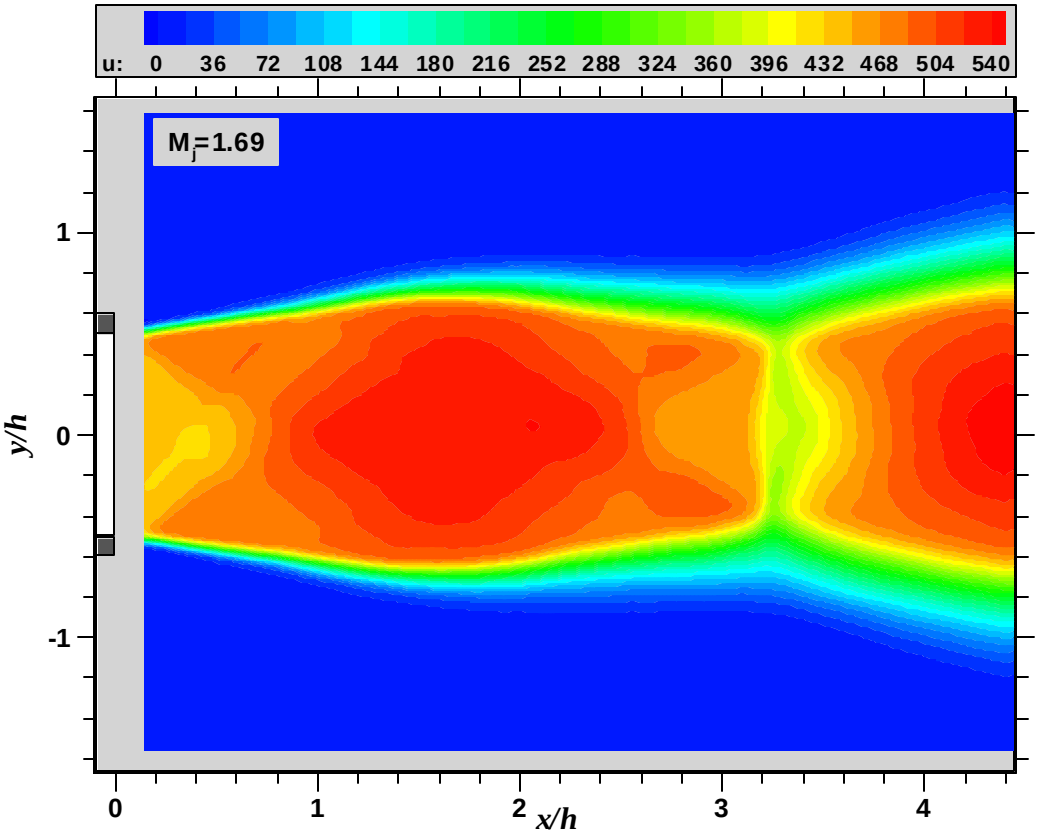

Figure 4. The mean *u* velocity field at the minor axis plane of the jet for M_j=1.69.

When the minor axis plane of the jet is analyzed, several features of an underexpanded jet can be easily identified. When the jet is operated with over pressure, an expansion fan originating from at the lip of the nozzle is observed. The angle of expansion of jet boundary at the exit can be calculated theoretically using Prandtl-Meyer function to give 7.4°, compared to measured angle of about 7.3°. This first expansion equalizes the jet pressure to the ambient pressure, up to a location where the expansion fan originating from the far side lip causes the jet to overexpand. Consequently, although for this operating condition the fully expanded jet velocity is 495 *m/s*, the jet expands up to 535 *m/s* in the first shock cell. When the expansion fan reaches to the opposite boundary of the jet, it reflects from the shear layer as a compression wave to keep the pressure unchanged. The reflecting compression waves form a compression region and the jet column starts to converge, while the jet velocity decreases. It is important to note that the flow velocity remains mostly unaffected at the boundary of the jet (or at the high velocity side of the shear layer), because the pressure and the total temperature remain

the same. In **Figure 4** a distinct slender region of low velocity can be identified at the end of the shock cell and may be misinterpreted as a shock if the flow field is not measured in the major axis plane.

When the flow field in the major axis plane is examined, compression waves reflecting from the two jet boundaries are observed to focus in the same region. The superposition of all these waves forms the low velocity region as mentioned. Although it is a significant compression, still it is not a normal shock, because the Mach number stays in the sonic regime. The source of the compression wave in the major axis plane is attributed to the side walls of the nozzle that are not contoured, but kept straight. In addition, the flow is not two dimensional for this particular aspect ratio even within the first or second shock cell.

In **Figure 5** the distribution of centerline velocity is shown and compared with pressure probe data. The pressure data combined with constant total temperature reveals the velocity by using the isentropic relations within the potential core or inviscid region of the jet. A very good agreement between the two data sets is observed except in the regions where the viscous effects begin to influence the probe measurements, such as the end of the shock cell. The first measurement point at the nozzle exit gives 442 *m/s* while the theoretical value is 445 *m/s* with a relative discrepancy of 0.7 %.

The mean density field in the minor axis plane is shown in **Figure 6** where an ensemble of about 100 realizations was used. These results are compared along the centerline with the density field computed from the velocity field data in conjunction with the total temperature T_t and isentropic relations. The results are shown in **Figure 7**. In order to calculate the spatially averaged data the velocity field measurements of major axis was averaged along the y direction within the potential core. Data shows that a reasonable agreement is achieved by the density field measurements.

The smooth variation of the density field within the shock cell shows that the compression waves do not coalesce enough to form a shock. Panda (1999) also noticed the smooth variation in his density measurements. He explained the smooth variation by the averaging effect of the fluctuations of the shocks. However, in the present study no

significant axial velocity fluctuation was measured within the potential core of the jet to have such an effect on the average profile.

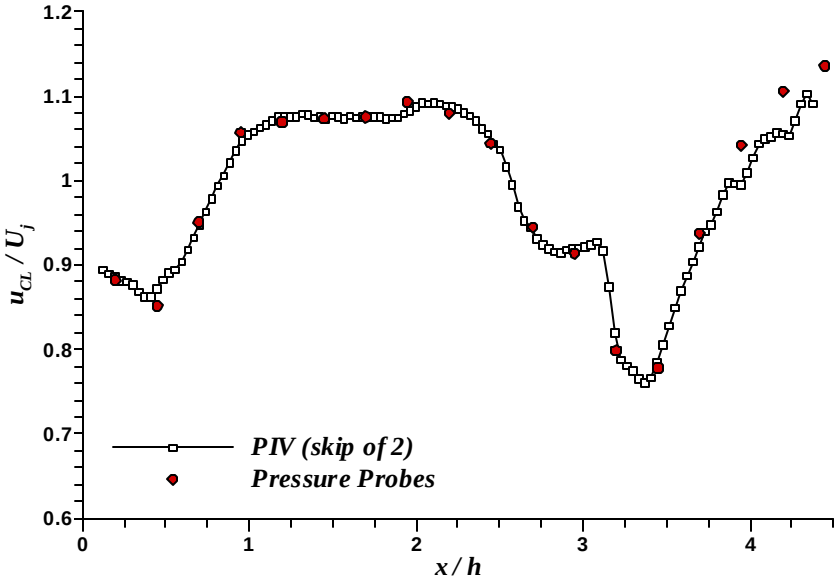

Figure 5. Centerline velocity distribution comparison of PIV and pressure probe measurements.

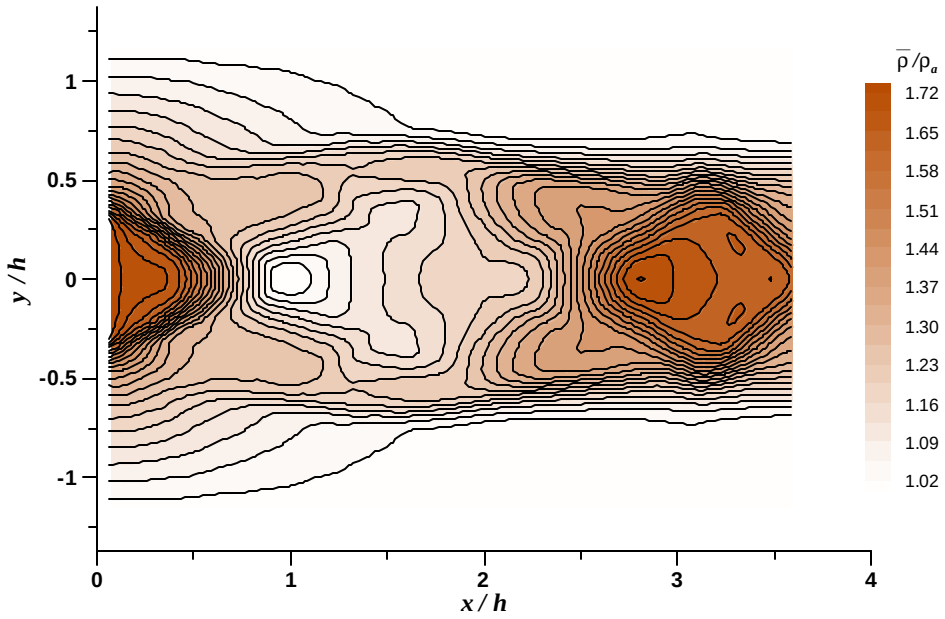

Figure 6. The density field measured by LSD at the exit.

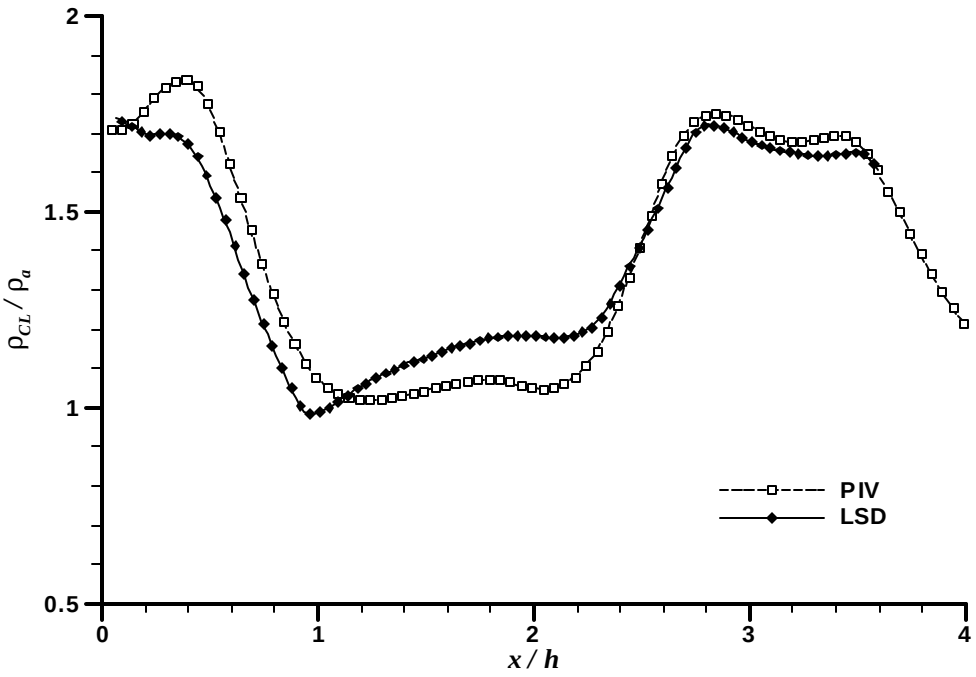

Figure 7. Density distribution along the centerline measured by LSD compared to the density calculated from the velocity field data using isentropic relations and the total temperature.

In order to bring out any effects of shock cell curvature, the velocity profiles in the minor axis plane were analyzed. In **Figure 8** the velocity profiles at downstream locations ranging from $0.5\,h$ to $4.5\,h$ are plotted. The velocity is normalized by the velocity jump in the shear layer and the transverse position is normalized by the vorticity thickness, d_w, found by the distance between the locations y_l and y_h, where vorticity is equal to 0.1 of $|w_z|_{\max}$ in both the low speed side and in the high speed side of the profile respectively. All of the normalized velocity profiles at downstream locations greater than $0.5\,h$, show some agreement and collapse to a unique profile indicating a geometric similarity. The profile is best represented by a Gaussian curve.

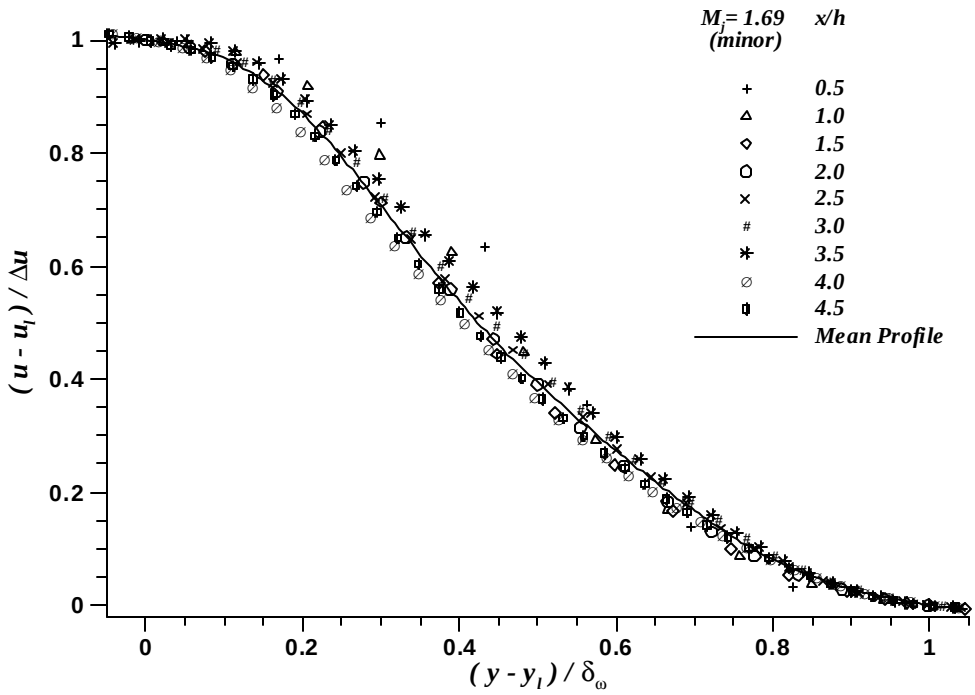

Figure 8. Profiles of dimensionless velocities in cross sections of the initial region of the jet at M_j = 1.69 (minor axis).

In **Figure 9**, the growth of vorticity thickness is shown for the initial region of the jet. The three regions are clearly identified by the slope change. These changes in the growth occur where the flow changes from expansion to compression or conversely when the flow starts to expand after a compression region. The growth rate of the vorticity layer at the two expansion regions in the first and second shock cell seems to agree with each other having the values of 0.11 and 0.09. In comparison, the compression region has a growth rate of 0.18, which is about two times the value of expansion regions. To our knowledge, this result was not observed before partly due to lack of data at such precision and grid density, and partly due to the few experiments done with improperly expanded jet shear layers. The changes in the growth rate cannot be attributed to the compressibility effects, since the properties at the high-speed side of the

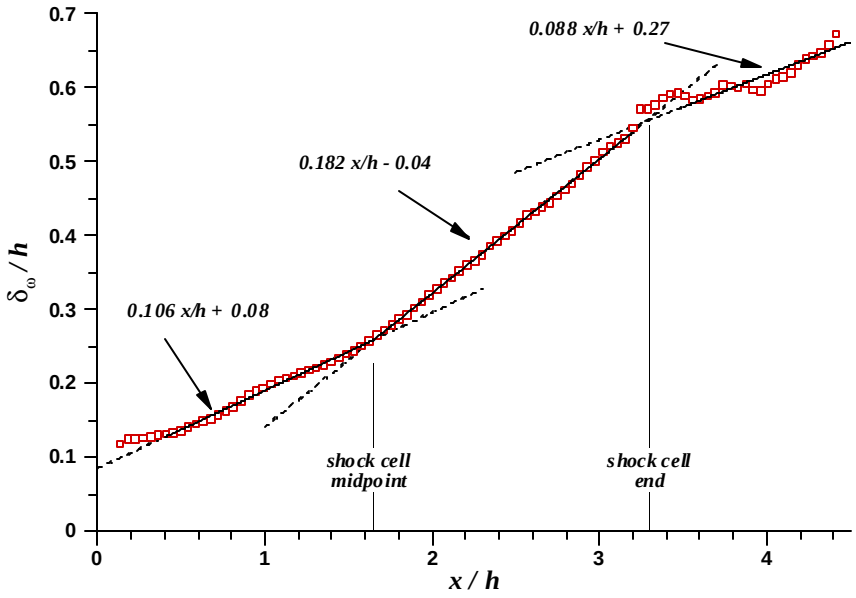

Figure 9. Shear layer growth at M_j =1.69 in the initial region.

shear layer should not change within the potential core. In contrast to considerable change in centerline velocity, u_{CL}, velocity at the high speed side of the shear layer, u_h, attains its value within 4 % of the fully expanded jet velocity, U_j, except at the shock cell end.

The results obtained in these detailed measurements reveal some new information about the shock cell structure and initial shear layer characteristics at the boundary of shock cells seen in improperly expanded supersonic jet flows.

References

Alkislar, M. B., "Flow Field Measurements in a Screeching Rectangular Jet", *Dissertation*, 2001, Florida State University, Tallahassee.

Köpf, U, "Application of Speckling for Measureing the Deflection of Laser Light by Phase Objects", *Optics Communications*, n.5, pp.347-350, 1972.

Krothapalli, A., Alkislar, M. B. and Lourenco, L., "The Role of Large Scale Structures on the Screech Amplitude", *AIAA Paper* 01-2144, May 2001, Maastrich.

Lourenco, L., and Krothapalli, A. "Mesh-free, second order accurate algorithm for PIV processing", *International Conference on Optical Technology and Image Processing in Fluid, Thermal and Combustion Flow*, 1998, Yokohama Japan.